JOURNAL OF MATERIALS SCIENCE 29 (1994) 5047–5053

Microscopy of impact damage in particulate-filled glass–epoxy laminates

G. PRITCHARD, QIANG YANG
School of Applied Chemistry, Kingston University, Penrhyn Road, Kingston upon Thames KT1 2EE, UK

Low-energy impact damage was induced in particulate-filled glass–epoxy laminates by means of a falling weight device, and the damage features were studied by sectioning through the impacted area. The polished sections were studied by optical and scanning electron microscopy to obtain comparative qualitative information about the effects of several different mineral fillers: solid glass beads, hollow glass microspheres, quartz, alumina trihydrate and mica. Approximately 8.5 mm thick laminates, with and without fillers, were impacted at various energies up to 43 J. At the lower impact-energy levels, the damage in the unfilled laminates in most samples was typically transverse matrix cracking, at some distance below the point of impact. Transverse and interlaminar cracking was more extensive in filled than in unfilled laminates. The type and distribution of the damage features are discussed in terms of the properties of the filler particles, and of the stress distributions involved.

1. Introduction

Fibre-reinforced organic-matrix laminates can sustain serious damage as a result of low-velocity transverse impact. The damage is not always obvious without close inspection, but there is often extensive intra-ply matrix cracking, and sometimes there is inter-ply delamination. At low energy levels, the damage usually takes the form of fine cracks in the matrix. These cracks by themselves have little effect on the bending stiffness or the load-carrying capability of laminates [1]. The residual strength of impacted composites decreases noticeably only when the cracks have sufficient energy to propagate and cause delamination [2]. When particulate mineral fillers are incorporated in laminates, for example as fire retardants, weight reducers, cost reducers or electrical property modifiers, the impact damage pattern becomes very complicated. Multiple delaminations can sometimes be observed along the interfaces between layers. (The extent of adhesion between the fibres and the filled resin is dependent on the nature of the filler, especially at high filler volume fractions where filler particles are observed in close proximity to the fibres.) There are again matrix cracks, and a certain amount of interfacial debonding of the filler particles from the organic matrix.

Crack initiation in particulate-filled glass–epoxy laminates usually occurs readily because of the high stress concentrations around the more angular particles, and around the broken fragments of any particles with low crush strength. In some cases, crack growth is later stopped by neighbouring particles because there is not enough energy for the crack to propagate either through or around them. Perhaps it is for this reason that particulate-filled laminates are more resistant than unfilled ones to the intra-ply delaminations which normally result from the accumulation of microcracks. In this context, the term intra-ply delaminations applies chiefly to those delaminations occurring at crossovers between 0° and 90° filament bundles originating within the same layer of woven roving reinforcement, or between parallel groups of filaments in warp or weft bundles. On the other hand, if there is sufficient energy for propagation around or through filler particles (and this depends on the kind of filler used) then intra-ply delamination can still be induced [3].

The objective of this research was to obtain qualitative evidence about how particle parameters influence the impact damage inflicted on woven roving glass–epoxy laminates. The test panels were subjected to low energy, low velocity drop-weight impact and then sectioned through the damage zones for microscopic examination. The type and extent of damage were subsequently observed and characterized.

2. Experimental procedure

2.1. Materials

The epoxy resin was supplied by Stag Polymers and Sealants (West Drayton, UK) under the trade name Epikote 816. This resin consists of the diglycidyl ether of bisphenol A together with a reactive diluent. The curing agent was 5 parts of piperidine (Merck, UK) per hundred parts of resin by weight. The fillers were as follows: untreated, easily crushed, hollow glass spheres with a very low wall thickness of 1.1 μm; silane-treated spherical glass beads; cleaved high-aspect ratio mica with low bulk density; and hard, irregularly shaped, untreated quartz particles (all sup-

0022–2461

TABLE I Characteristics of particulate fillers

Property	Glass beads	Hollow glass spheres	Alumina trihydrate	Mica	Quartz
Median particle size (μm)	15	35	15	20	15
Particle shape	Solid spheres	Hollow spheres	Crystalline hexagonal plates	Thin highly delaminated flakes	Crystalline hexagonal plates
Specific density ($g\ cm^{-3}$)	2.48	0.23	2.42	2.9	2.65
Bulk density ($g\ cm^{-3}$)	1.5	0.15	0.8	0.145–0.640	0.944
Mohs hardness	5.8	–	2.5–3.5	2.5–3.0	7
Surface treatment	Silane	None	None	None	None

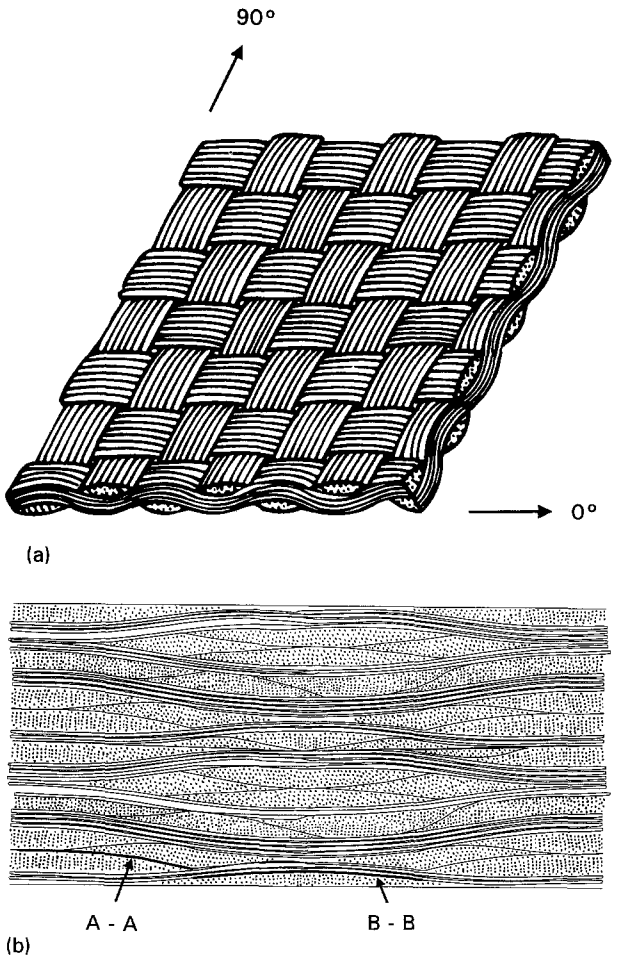

Figure 1 (a) The structure of the woven roving fabric. (b) Schematic diagram of the cross-section of a woven roving glass–epoxy laminate showing two typical interfaces.

plied by Croxton and Garry Ltd, UK) together with untreated angular alumina trihydrate (ATH) with relatively low hardness (Alcan Chemicals, UK). The characteristics of the particulate fillers are summarized in Table I. Woven roving glass fibre reinforcement (Fothergill and Harvey, Littleborough, Lancs, UK) with a warp:weft ratio of 60:40 was used to make 8-ply flat panel laminates by hand lay-up. The structure of the plain-weave fabric is shown in Fig. 1. The flexural strength and modulus of the cast filled and unfilled resins, and the tensile properties of the filled and unfilled laminates, were determined and will be the subject of a separate paper. The compressive properties have already been reported [4].

2.2. Laminate production

A steel plate 360 mm × 300 mm was coated first with a mould release agent (Rocol M. R. S. non-silicone dry-film spray) and then with a thin coating of the catalysed epoxy resin. The desired epoxy–filler mixture was poured on to the plate, followed by the woven roving fabric (approximately 50:50 w/w resin:glass fabric) and a hand roller was used to impregnate the fabric. The warp of the woven roving sheets was always kept in the same direction. During curing, slight contact pressure was applied to the laminate by means of a very heavy metal plate. Oven cure was carried out at 120 °C for 16 h. The nominal glass content was checked, being estimated by calculation from the known resin:filler ratio, after burning off all the resin by heating in an electric muffle furnace at 600 °C. Allowance was made for volatile losses from the filler (for example, ATH loses water by endothermic decomposition at less than 200 °C). The fibre volume fraction was about 0.25 in all cases.

2.3. Impact application

Single impacts were applied using the simple instrumented apparatus shown schematically in Fig. 2. A steel impactor of variable mass was fitted with a 20 mm diameter hemispherical steel nose and allowed to fall freely from a height of 1 m on to a flat-panel laminate specimen measuring 178 mm × 210 mm. Six

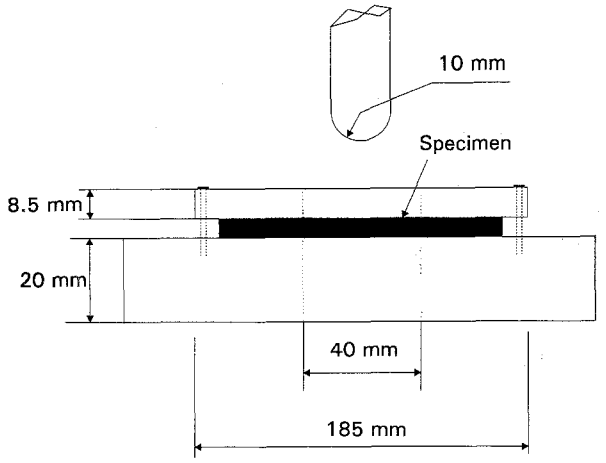

Figure 2 Schematic diagram of the drop-weight impact test apparatus.

kinetic energy levels were used: 14, 22, 29, 34, 39 and 43 J. The specimen support rig consisted of two thick steel plates, both having a central hole of 40 mm diameter. The test panels were rigidly clamped between the two steel plates to form a sandwich and impacted at their centres.

2.4. Damage examination

Acoustic emission of some of the highly filled laminates gave rather unsatisfactory results in some cases and so the damage was assessed instead by direct microscopic examination of cross-sections, together with measurements of the retention of mechanical properties; the latter aspects were discussed elsewhere [4]. The samples were sectioned across their damage zones (Fig. 3). They were ground with a rotary belt sander using carbide abrasive paper (166 grit) until smooth, and polished using silicone carbide abrasive papers of successively finer grit sizes (240, 600, 1000) on a rotating grinding wheel. Running water was used to remove any dust produced and to minimize frictional heating. The various cross-sections of the damaged laminates were subsequently inspected and photographed using an optical microscope at magnifications of between 7 and 20. The maximum length of the damage zone was measured under the optical microscope. The polished surfaces were later coated with gold for examination by scanning electron microscopy (SEM) to obtain evidence of the extent of

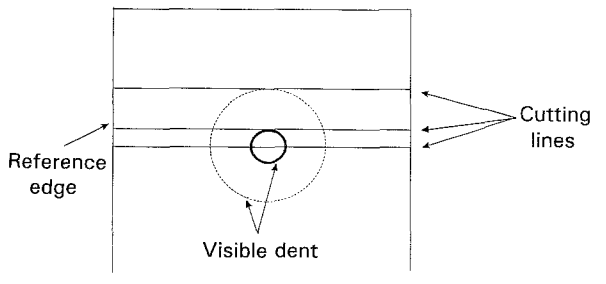

Figure 3 Schematic diagram showing cross-sectioning through the impact damage zone.

fibre–matrix debonding, fibre pull-out, and the crack initiation and propagation processes, as well as to study the role of the filler particles.

3. Results and discussion

3.1. Damage to the surfaces

Casual visual inspection of the damaged specimens indicated some common features. Slight permanent indentations were visible on the top (impacted) surfaces. The indentations became deeper at greater impact energies. Corresponding domed areas on the unimpacted (lower) surfaces of the specimens were observed after impact, except for the mica-filled samples, on which unusually extensive matrix cracking appeared instead. When the impact energy was increased to 39 J, fractured glass fibres were observed on the unimpacted surfaces of the glass bead samples. No such fractures were observed with the other fillers at the same impact energy level. The first reason to be considered for this unique glass bead behaviour was high filler-to-resin adhesion, partly because of silane treatment (the other fillers were untreated). There might also be improved filler–matrix adhesion because of the surface smoothness of the beads, facilitating good contact with the liquid resin. The strong interfaces thus generated would inhibit particle–resin separation and prevent matrix cracking from propagating to induce delamination [5, 6]; the impact energy would be dissipated in fibre breakage instead.

This argument was later rejected. Other considerations suggest that despite microscopic evidence of some limited debonding of filler particles, filler-to-resin adhesion should be fairly good with almost all of the particles, not just glass beads, whether the particles are surface-treated or not. Interfacial bond strength is provided by the compressive forces generated during cure as a result of the mismatch in thermal expansion coefficients of resin and filler [7–9]. Also, glass beads are far from unique in possessing surface polar groups capable of contributing to interfacial adhesion with epoxy resins.

A more plausible explanation is that the intrinsic strength of glass beads is higher than that of hollow glass microspheres with their weak walls, or ATH or mica particles with their planes of weakness and inherent microdefects. Therefore the energy contained in the propagating cracks is not easily spent in fracturing glass beads; it is still available to fracture fibres. The glass fibres most likely to break are those which by virtue of their position on the outer surface of the laminate are subjected to high bending stresses during the mechanical deflection of the sample immediately after contact with the indentor. There remains the question of why the residual crack energy is spent in breaking fibres, rather than in promoting delamination. Very few fibres were observed to be fractured except with glass beads. Presumably delamination is easier with the other fillers than with glass beads, and this in turn implies that the glass bead-filled epoxy resin adhered better to the fibres than the other fillers. The short-beam interlaminar shear strength of the glass bead-filled laminates was determined and found

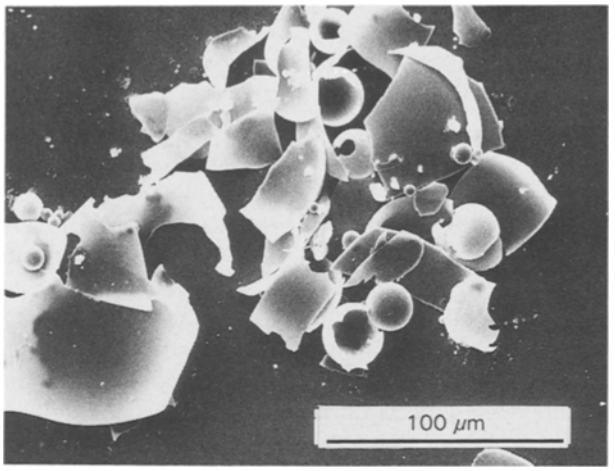

Figure 4 Scanning electron micrograph of fragments of the broken hollow glass spheres.

to be slightly higher (40.3 MPa) than that of the quartz (37.4 MPa) and much higher than that of the ATH-filled samples (27.9 MPa).

Casual inspection of the major surfaces of hollow glass microsphere-filled laminates displayed no externally detectable damage, other than the previously mentioned small permanent indentations after impacts of up to 29 J. Nevertheless considerable internal damage was sustained, mostly through the crushing of the microspheres (Fig. 4) and through plastic deformation of the epoxy resin already implied by the deformations. The spheres used were exceptionally thin-walled compared with some other grades available commercially which might be expected to behave differently.

3.2. Through-thickness damage

Optical micrographs showed that all the impacted panels, except those containing hollow glass microspheres and mica, exhibited similar impact modes, typical of brittle materials. Damage initiated in one of three possible locations. One was on the top surface near the impact point, where damage was induced by contact stress, as with mica; another was close to the edges of the 40 mm hole in the two specimen support plates, where shear stress-induced transverse matrix cracking occurred, and the third was on the lower surfaces beneath the impact point, where cracks appeared because of flexural deflection. In most cases the main damage zone region was conical, with the widest part of the cone on the lowest surface furthest from the impact point. The size of the cone depended on the level of incident impact energy and on the filler.

Apart from the mica-and hollow glass microsphere-filled laminates, there was a clear division between specimens with no readily visible matrix cracks or delaminations, and those with readily visible matrix cracks which delaminated extensively, the affected region becoming wider as the impact energy increased. Delaminations occurred along the interfaces between the 90° fibre bundles, and at 0°–90° interfaces. (Refer to Fig. 1 for the definition of direction; typical delaminations are indicated in Fig. 1 as A–A and B–B for 90° and 0°–90° respectively, propagating away from the centre of the impacted area.) These observations support the view that matrix cracks constituted the first significant failure mode in woven-roving laminates. Delaminations then followed, once the cracks had propagated as far as the interfaces with plies of different orientations (0°–90°) or between adjacent 90° fibre bundles.

3.3. Unfilled glass–epoxy laminates

A close inspection of the cross-sections of the impacted glass–epoxy laminates showed that unfilled laminates suffered less matrix cracking and fewer delaminations than any of the filled ones at all energy levels. Very few matrix cracks were observed in the lowermost 90° ply of unfilled laminates after an impact of 14 J. These bending-induced tensile cracks indicated that the lower surface was subjected to tensile stresses exceeding the failure stress of the matrix. Static tensile tests showed that the tensile strength of the unfilled resin was 82 MPa and its elongation at break was 4.9%. When particulate mineral fillers such as ATH were added to the resin, the tensile strength and elongation at break both decreased sharply (Table II). As the impact energy increased to 34 J, transverse shear matrix cracks (Fig. 5) and bending-induced tensile cracks occurred throughout the thickness of the laminates. At impact energy levels of more than 39 J, some of the transverse shear cracks propagated through the 90° plies and extended into the interlaminar region, inducing delaminations (Fig. 6). But these delaminations were stopped by the interfaces between 0° plies and could sometimes be halted by a void on the interface if they lacked enough energy to break through or circumvent it (Fig. 7).

3.4. Alumina trihydrate

Damage was detected between the 90° layers in the lower laminae after an impact energy of only 14 J. Matrix cracks were observed in the lower plies, as a result of the flexural response of the beam on impact. Slow-bend experiments were performed and they induced the first matrix cracking in the tensile lower faces at a mid-point deflection of 2.2 mm when the span was 140 mm and the thickness was the usual

TABLE II Tensile strength and elongation as a function of ATH content

ATH content (php)	Tensile strength (MPa)	Elongation (%)	Tensile modulus (GPa)
0	82 (2)	4.9 (0.2)	3.2 (0.2)
20	63 (2)	2.2 (0.1)	3.9 (0.3)
40	61 (2)	1.8 (0.1)	4.9 (0.3)
60	58 (4)	1.4 (0.2)	5.9 (0.4)
80	48 (6)	0.9 (0.2)	6.1 (0.3)
100	55 (4)	0.9 (0.2)	6.8 (0.4)

Standard deviations are in brackets.

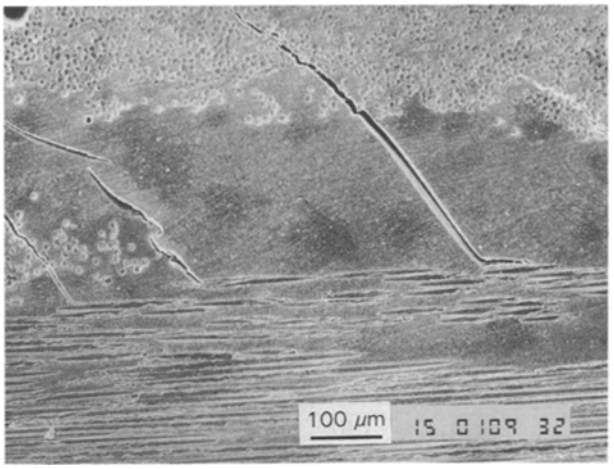

Figure 5 Scanning electron micrograph of impact-induced transverse cracking in an epoxy–glass woven roving laminate.

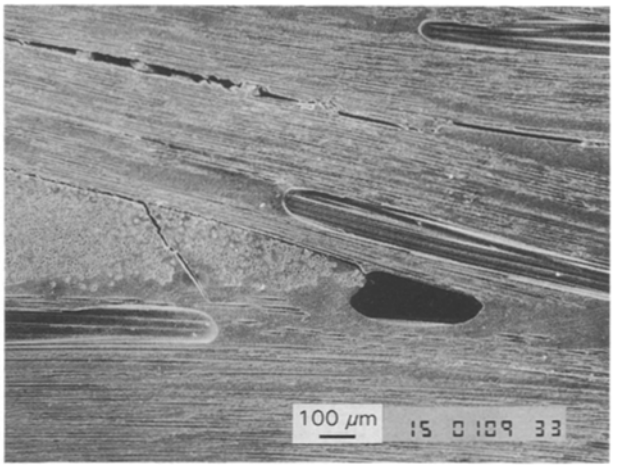

Figure 7 Scanning electron micrograph showing the termination of delamination by a void on the interface of epoxy–glass woven roving laminate.

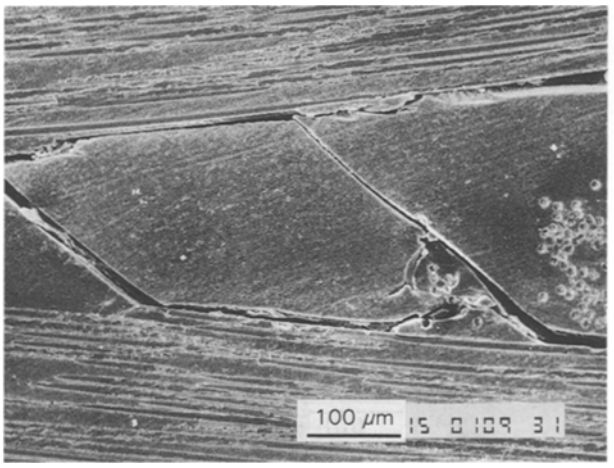

Figure 6 Scanning electron micrograph of intra-ply transverse cracking and delaminations at 0°–90° interfaces of epoxy–glass woven roving laminate.

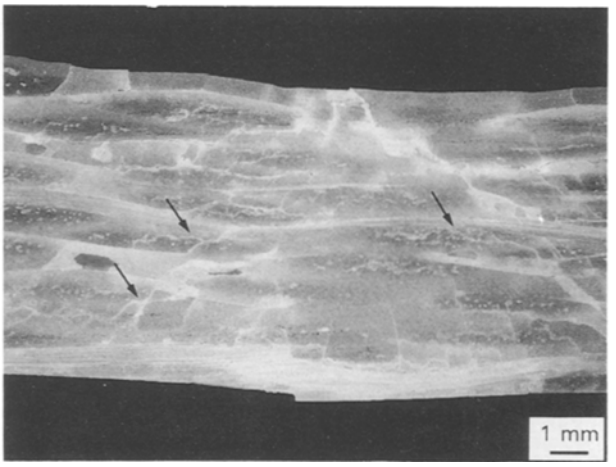

Figure 8 Optical micrograph of a quartz-filled epoxy–glass woven roving laminate (100 parts quartz per 100 parts of epoxy resin by weight) after an impact of 39 J. Arrows indicate typical cracking on the lower (unimpacted) face, and matrix cracks in the adjacent plies.

8.7 mm. The validity of any comparison between slow-bend conditions and fast-impact loading must be uncertain as the strain rates were quite different.

3.5. Quartz

The same damage pattern was reproduced in the glass–epoxy–quartz laminates, but quartz-filled samples gave a better impact resistance at impact energies of 14 and 29 J than ATH. In contrast, however, quartz-filled laminates exhibited considerably more impact damage at the higher impact energies than ATH samples. For example, at more than 34 J, cracking extended throughout the thickness of the laminate. Fig. 8 shows typical impact damage in a 100:100 w/w quartz:epoxy–glass laminate sample after an impact of 39 J. The majority of the visible damage consists of matrix cracks on the lower face. A conical zone of sheared fibres was observed in this micrograph. This can be attributed to the hardness of quartz. Matrix flexibility was greatly decreased by the incorporation of quartz particles with their high modulus into the epoxy resin. Consequently, there was less opportunity for impact energy to be dissipated in plastic deformation and it was spent instead partly in shearing fibres.

3.6. Mica and hollow glass microspheres

Mica behaved quite differently from the other fillers. Matrix cracking and delaminations were detected in the upper plies after impact at 14 J or higher energies. This contrasts with most other fillers where the main damage focus was near the unimpacted surface. Closer examination of the impact zone suggested that the matrix cracks had initiated at the edge of the area of impact, as a result of the contact stress field. The mica-filled laminates were the most susceptible of all to impact damage. At all impact energy levels, extensive delamination occurred, with minimal matrix cracking. Fig. 9 shows only half of a specimen which has been impacted (39 J) from the side with gross delamination. The specimen was a laminate having 50 parts of mica per 100 parts by weight of resin. Delamination was

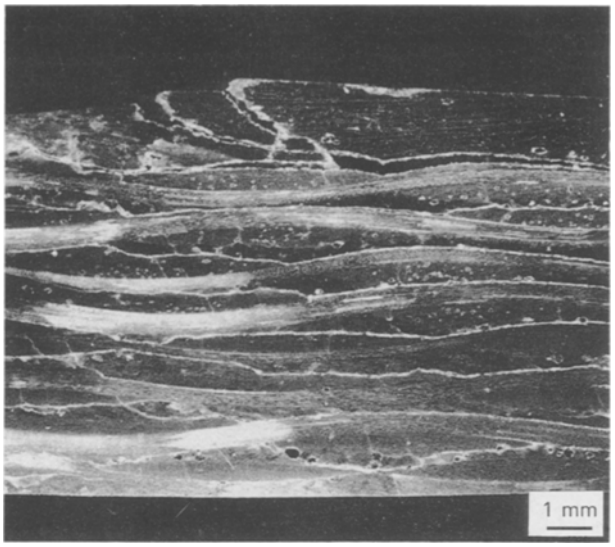

Figure 9 Optical micrograph of a mica-filled epoxy–glass woven roving laminate (50 parts mica per 100 parts resin by weight) after an impact of 39 J. Note the delaminations near the upper (impacted) face where the impact occurred.

more severe near the impacted surface, probably because of severe transverse shear stresses. The weak interface between fibres and matrix would be expected to facilitate delamination.

3.7. Solid glass beads

A side view of the cross-section of the damage zone in solid glass bead-filled laminates is shown in Fig. 10. There are matrix cracks aligned at about 45° to the impact direction, one of which is marked by a letter C on the figure. These cracks are not directly beneath the impacted area, but some distance away; the shape of the affected region always appears conical. Up to 29 J, flexural failure occurred in the lower surface region, as shown with a letter D in Fig. 10. However, delaminations were found in glass bead-filled laminates only at the highest impact energy used, i.e. 43 J. This can be explained by the greater energy requirement for delamination arising from better adhesion of the glass bead–epoxy matrix to the fibres. It is also worth considering the stress distribution. The glass beads were spherical, and they induced lower stress concentrations around them than the more angular particles such as quartz. This discouraged the formation of critical matrix cracks of the kind which normally lead to multiple delaminations. Incidentally, a small number of approximately spherical voids were observed in the matrix and they acted as crack stoppers by crack blunting.

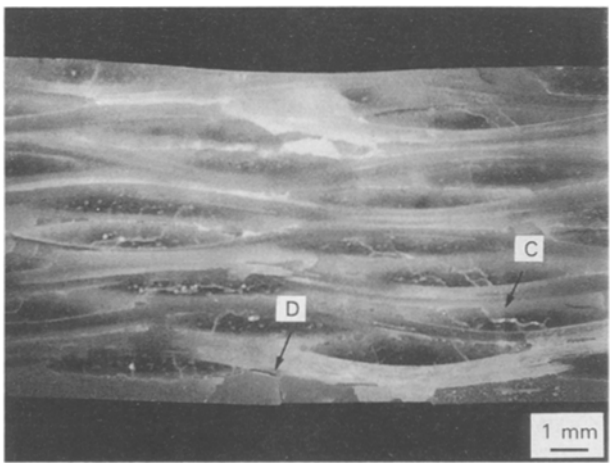

Figure 10 Optical micrograph of a glass bead-filled epoxy–glass woven roving laminate (100 parts glass bead per 100 parts resin by weight) after an impact of 29 J. Note the typical matrix cracking (C) on the lower parts and the flexural failure (D) on the lowermost ply.

3.8. Comparisons between the five fillers

The behaviour of the various fillers is summarized diagrammatically in Table III. It is not proposed that the observations found would necessarily be repeated with fillers of the same composition but different particle size distribution, surface treatment etc. The results are specific to the filler grades used here. Nor is it possible to be dogmatic at this stage about any of the above suggested interpretations. Each filler has a family of characteristics and complete isolation of variables is not possible with a comparative study of this kind.

Each filler has its own characteristic impact-induced damage modes. It is apparent that the 90° fibres are prone to intra-ply matrix cracking, because of out-of-plane bending stresses induced by impact. Unfilled glass–epoxy laminates showed the best resistance to impact damage, and had the smallest damage zones in all cases. This can be attributed to their having lower stress concentrations and fewer weak interfaces than filled ones. The hardest filler, quartz, induced a larger damage area and more severe damage (shear-fractured fibres) at higher impact energies than ATH samples. It is probable that the difference in the hardness or modulus (see Table I) of these two fillers is the reason for their different impact behaviour. It was observed from routine mechanical measurements that the addition of hard fillers, such as quartz, increased the matrix flexural modulus greatly and therefore improved the ability to resist low-energy impact. On the other hand, as the applied impact energy increased, fibre breakage occurred more readily in the quartz samples because the impact energy was not absorbed by elastic or plastic deformation. It was dissipated by fibre fracture instead. Mica and hollow glass spheres caused the most significant reduction in impact damage resistance of laminates. Mica particles have an easily delaminated structure and an irregular shape. The first feature produces relatively weak interfaces between laminae, easily broken by impact-induced shear stress. The second feature induces stress concentrations at which cracks are initiated.

The hollow glass spheres with their low wall thickness of only 1.1 μm have a very low crush strength. Although the spheres themselves promote a relatively low and uniform stress concentration, once broken the glass fragments formed during impact constitute larger stress concentrations, and hence initiate crack-

TABLE III Summary of the effects of the fillers on the impact damage

Filler type	Effects at 14 J	First delaminations at	Special features
Hollow glass spheres	No visible surface damage	22 J between the middle plies	Particle fragmentation
Glass beads	A few matrix cracks throughout the thickness	43 J at the interfaces between 90° fibre bundles of lower plies	Broken fibres on reverse side
Quartz	Very few matrix cracks throughout the thickness	34 J in lower plies	A conical zone of sheared fibre through the thickness
ATH	Matrix cracks in lower plies	29 J at the interfaces between 90° fibre bundles	Extensive matrix cracks on unimpacted surface
Mica	Matrix cracking and delamination in upper plies	14 J throughout the thickness	No domed area on reverse face

ing in laminates. The major impact-induced damage mode is debonding between fibres and matrix (taking the word matrix to include both resin and filler together) and interfacial adhesion is therefore important. We assume that weak interfaces were formed in mica- and hollow glass sphere-filled laminates because of the very poor wettability of the glass fabrics by a matrix of epoxy resin highly filled with mica or hollow glass spheres. This can be explained by these fillers having low bulk densities and by their imparting comparatively high viscosities at a given filler loading. High viscosities make it difficult to achieve perfect impregnations and some weaker interfaces resulted. Among the five fillers, glass beads gave the least damage at all impact energies. The chief reason is believed to be their intrinsic strength, but minor contributions may be made by their favourable spherical shape and the resistance they provide to delamination. The benefits of glass beads are achieved at the cost of fibre breakage in the ply remote from the impact point, at the higher end of the energy range.

4. Conclusions

1. All the fillers caused a deterioration in the impact damage performance of woven-roving glass fibre–epoxy laminates.

2. The area of the damage zone, assessed by measuring the observed damage on the surface or through the thickness, was increased by the addition of particulate fillers.

3. Incorporation of particulate fillers into laminates resulted in greater stiffness and accentuated the likelihood of initial matrix cracking during momentary deflections at a given low impact energy. It facilitated fibre breakage at high impact energy.

4. When weak fillers with low crush strength and low bulk density were added, delamination rather than matrix cracking became the dominant damage mode at all impact energies.

5. The particle shape had a small, but noticeable, effect on impact damage. Spherical particles required increased impact energy to generate the stress concentrations required to initiate delamination in laminates.

Acknowledgements

Q. Yang acknowledge financial support from Kingston University during the course of research. Both authors thank Dr A. Bandara and Mr P. Spearman of Kingston University for their help in designing and constructing the drop-weight impact apparatus and developing the software. We also extend our appreciation to Alcan Chemicals Ltd, Gerrards Cross (UK) and Croxton and Garry Ltd, Dorking (UK) for supplying fillers.

References

1. L. W. GAUSE and L. J. BUCKLEY, in ASTM STP 936 (American Society for Testing and Materials, 1987) p. 248.
2. T. TAKEMORI, *J. Mater. Sci.* **17** (1982) 164.
3. R. WAINWRIGHT and G. PRITCHARD, "The properties of epoxy resins containing alumina trihydrate filler", MOD report, Agreement No. D/ER1/9/4/2055/14 ARE (Kingston Polytechnic, 1988).
4. G. PRITCHARD and Q. YANG, in Proceedings of FILPLAS'92, 5th International Fillers Conference and Exhibition, Manchester, UK, 19–20 May 1992, British Plastics Federation and The Plastics and Rubber Institute (BPF/PRI, Manchester, UK, 1992).
7. B. CORNWALL and V. D. KRSTIC, *J. Mater. Sci.* **27** (1992) 1217.
8. M. OCHI, K. YAMASHITA and M. SHIMHO, *J. Appl. Polym. Sci.* **43** (1991) 2013.
9. C. F. FAN and S. HSU, *J. Polym. Sci.* **30** (1992) 603.

Received 8 November 1993
and accepted 19 January 1994